Densified Collagen Tubular Grafts for Human Tissue Replacement and Disease Modelling Applications

Alexander W. Justin[1*], Sebastian Burgess[1], Silas R. Estevez[1], Agavi Stavropoulou-Tatla[1], John Ong[1,2], Aishwarya G. Jacob[3], Kourosh Saeb-Parsy[4], Sanjay Sinha[5], Athina E. Markaki[1*]

[1]Department of Engineering, University of Cambridge, Trumpington Street, Cambridge CB2 1PZ, UK.

[2]East of England Gastroenterology Speciality Training Program, Cambridge, UK.

[3]Wellcome-Medical Research Council Cambridge Stem Cell Institute, Anne McLaren Laboratory, University of Cambridge, Cambridge CB2 0SZ, UK.

[4]Department of Surgery, University of Cambridge, and NIHR Cambridge Biomedical Research Centre, Cambridge, CB2 0QQ, UK.

[5]Department of Medicine, Division of Cardiovascular Medicine, University of Cambridge, Cambridge CB2 0QQ, UK.

Corresponding Authors: Dr Alexander W Justin (awj27@cam.ac.uk)
Dr Athina E Markaki (am253@cam.ac.uk)

ABSTRACT

Fabrication of tubular grafts *de novo* has been limited by the ability to produce constructs which fulfil the mechanical and biological requirements for implantation and function. In this work, we present a novel method for the formation of densified collagen hydrogel tubular grafts on the scale of human-sized vessels. The seamless, densified collagen hydrogel tubes are highly customisable in terms of luminal diameter and wall thickness; here we report tubes with luminal diameters 1-5 mm and wall thicknesses of 0.2-3 mm. Using genipin as a biocompatible crosslinker, we eliminate the acid solubility and swelling of the collagen, while increasing the strength of the tubes. While the materials-based method of manufacture enables acellular grafts to be generated rapidly, the cell-compatible densification method enables a high density and uniformly distributed population of cells to be incorporated into the walls of the construct, as well as onto the luminal surface. Additionally, we report a method for generating tubes consisting of distinct cell domains in the walls. The cellular configurations at the boundary between the cell populations may be useful for disease modelling applications. We also demonstrate a method for luminal surface patterning of collagen tubes.

Keywords: Densified collagen, tissue engineering, vascular grafts, tubular scaffolds, disease modelling

1. INTRODUCTION

Tissue engineering seeks methods for the generation of bioengineered tubular grafts with superior clinical outcomes, leading to fewer surgical interventions and reduced demand for hospital access. This includes blood vessels (e.g. coronary and peripheral arteries, vascular access grafts for hemodialysis) [1-5], the bile duct [6, 7], small and large intestine [8-10], oesophagus [11, 12], genitourinary [13] and tracheobronchial [14-17] systems, and guiding conduits for peripheral nerves [18]. Researchers also seek artificial tissue for disease modelling *in vitro* [19-21], to reproduce vascular pathology in atherosclerosis [22] and Marfan syndrome [23], in which three-dimensional (3D) cell culture systems can recapitulate the native cell response in the extracellular matrix (ECM).

Bioengineered tubular grafts have been generated via processing of a wide range of materials, including synthetic materials (e.g. polyester, polyurethane), cadaveric tissue, or biomaterials such as collagen and fibrin, as well as scaffold-free approaches [23-25]. Scaffolds derived from decellularised cadaveric tissue [26], while providing a high degree of bioactivity and innate vascularisation, are limited in availability and customisability in terms of dimensions and composition. Synthetic-based scaffolds, while inexpensive and simple to manufacture, frequently lack the biological niche and degradation characteristics for cellular repopulation and remodelling. To overcome this, a common approach is to use cells, seeded upon a synthetic porous scaffold, to produce native ECM (e.g. human acellular vessels) [27, 28]. Ideally, we seek to generate implantable constructs without the use of cells during manufacture or in the final product, using fully definable, patient-derivable, and non-immunogenic biomaterials, which would yield a rapid and inexpensive method for off-the-shelf tubular grafts.

The method of generating bioengineered grafts may also be amicable to cell seeding both onto the surface and uniformly in the walls of the tissue for more complex tissue types, allowing for cellular remodelling, providing suitable and tuneable mechanical properties to match native tissue, and importantly be scalable from small animal models to human vessel dimensions. Tissue-specific challenges must also be addressed, such as thrombogenicity in blood vessels or acidity in urothelial conduits. Furthermore, many tissues will require the incorporation of organoids to recapitulate tissue function and so require a cell-compatible manufacturing process. Intestinal grafts also require fabrication methods to generate the high luminal surface area and rich vasculature necessary for physiological function.

Methods for producing collagen-based grafts specifically include freeze-drying (yielding mechanically weak and highly porous sponges) [8, 29], electrospinning (high density of collagen, limited cellular remodelling and infiltration) [30], or through a hybrid with synthetic materials in which the synthetic component provides the mechanical support for the collagen or ECM [31]. Alternatively, collagen hydrogel approaches support high bioactivity and consist of a macromolecular network of collagen fibrils which retain a significant volume of water. However, a standard collagen gel is mechanically weak and high collagen concentrations are difficult to deploy owing to high viscosity and rapid gelling times. Further, collagen fibrils are randomly orientated; in the native ECM, fibrils are hierarchically organised and aligned over distance which, alongside native crosslinking mechanisms, provide the tissue with mechanical support.

Several techniques [32-38] have been investigated to produce tubular collagen grafts by increasing the fibril alignment and density of a collagen hydrogel, thereby producing a mechanical robust construct while still retaining high bioactivity. This is achieved by removing a large fraction of the interstitial water from the hydrogel through ‘plastic compression’ [33, 35], air drying [38], rotation-based water loss [37], gel compaction driven by cell traction forces [34] or cyclic straining [32]. Collagen grafts have also been produced by the rolling of densified collagen sheets, but this leads to the formation of seams [36]. Many of the resultant tubes tend to be thin-walled [32, 34, 35, 37], failing to match the wall thickness of human vessels, and are not easily scalable to human-sized vessels.

We have developed a novel, materials-based method of manufacture for the formation of tubular densified collagen hydrogel grafts, which allows for densification in both the axial and radial directions using a funnel-shaped mould. This results in mechanically robust tubes which are widely customisable in terms of tube diameter and wall thickness. Tubes can be manufactured acellular, or cellularised by uniformly seeding cells into the walls of the conduit prior to collagen gelation and densification, or by seeding cells onto the luminal surface after the densification process is complete. Furthermore, the densification method is applicable to both small animal and human-sized conduits. To stabilise the collagen structure against acid degradation (e.g. urea) and to closer match the mechanical strength of real tissue, we further crosslink the densified collagen tubes using genipin, a naturally occurring (biocompatible) crosslinking agent, which can be used in the presence of embedded cells. Additional steps to the standard technique enable more niche and disease modelling applications to be targeted. The shape of the funnel can be used to produce constructs with a gradient collagen concentration along their length. By casting collagen in sequential steps, one can produce tubes with distinct cellular domains, which may be useful in disease modelling involving boundaries between cell types. Indeed, we show a spatial organisation of cells near the boundary which is highly reminiscent of the organisation of smooth muscle cells (SMCs) in the proximal aorta (neural crest and lateral plate mesoderm origins) and thus may be useful for studying aortic aneurysms. Additionally, ultra-fine conduits can be generated using pre-densified constructs and applying an additional air-drying step. Finally, a method has been developed for patterning the luminal surface which may support the future generation of intestinal crypt-villus structures.

2. MATERIALS AND METHODS

2.1. Materials

Collagen solution was generated from rat tail tendons using a known method [39]. Briefly, frozen rat tails were purchased (Blue Lizard Reptiles) and the tendons excised. Following 72 h in 0.02 M acetic acid solution at 4 °C, the solution was centrifuged at 7500 g for 90 min and freeze-dried. After weighing the dry mass of collagen, it was resuspended at 10 mg/mL in 0.02 M acetic acid solution and stored at 4 °C.

Collagen gel was generated using an established method [40]. Briefly, for preparation of 2.5 mg/mL collagen precursor solution (60 mL), the reagents used were: 10x M199 medium (Sigma, 2 mL), 1 M NaOH (Sigma, 0.250 mL), stock 10 mg/mL collagen solution (10 mL), sodium bicarbonate solution (Sigma, 0.6 mL), penicillin-streptomycin (Sigma, 0.2 mL), amphotericin-B (Sigma, 0.2 mL), and cell medium (6.75 mL). Viscous collagen solution was transferred using a 10 mL syringe and added last. The solution was shaken vigorously until thoroughly mixed and centrifuged at 4000 g for 10 min at 4 °C.

Perspex chambers, for casting and collagen densification, were machined to tube specifications, consisting of a funnel section and cylindrical section, and a flange base. The internal surfaces were polished to remove machining marks. Additionally, top and bottom jig pieces were machined from Perspex, and Perspex, PTFE and nylon rods were purchased to size (Engineering & Design Plastics). Nylon membranes were used with pore sizes of 1.2 µm and 0.45 µm (Millipore).

2.2. Manufacturing method

Perspex funnels and additional components were immersed in ethanol and dried prior to experiments. Internal funnel surfaces were coated in sunflower oil using paper towels and positioned upside down. A ring of dental silicone (Billericay Dental Supply Co.) was placed around the central hole and a 1.2 µm nylon membrane was positioned over the hole. A machined, Perspex jig was placed over the chamber flange to flatten the membrane and silicone. A locating hole at the

centre of the jig provided alignment in the centre of the casting chamber for a biopsy punch (Agar Scientific) which produced a hole to match the diameter of the central rod (e.g. 2 mm, 5 mm). The jig was then removed and additional 0.45 and 1.2 µm membranes were fixed over the top, using the jig once again to flatten the silicone and membrane. Membranes and funnel were subsequently pre-wetted with sterile phosphate-buffered saline (PBS, Sigma) to liberate any trapped air bubbles between the membranes. Collagen precursor solution was prepared as described above and transferred to the funnel. An unsupported, water-impermeable polystyrene sheet can be placed under the membranes to prevent early leakage of the collagen precursor solution prior to gelling.

The collagen solution was visibly clear of air bubbles after centrifugation. Failure to remove all the bubbles led to sub-optimal tubes with high numbers of defects or could disrupt the densification process entirely. The collagen solution was poured very slowly down one side of the internal funnel surface, thereby preventing any mixing of the oil and collagen solution and preventing any turbulence which may trap air bubbles. The pre-wetted membranes allow the infiltration of collagen solution, which subsequently provided a gripping point for the collagen gel. Once the whole collagen solution was in the funnel, the central rod was slowly lowered into the chamber and interlocked into the locating hole in the top membrane, providing alignment to the rod from below. A second Perspex jig provided central alignment from above.

The whole assembly was then left in a 37 °C incubator for 1-2 hours to allow the collagen to gel. Following this, the funnel assembly was subsequently positioned on top of wetted towels. The full assembly was then placed in a 37 °C incubator, or under a biological cabinet at room temperature, for 2-24 h for the collagen gel to densify. After densification, the densified collagen tube was carefully extracted from the cylindrical section and subsequently stored in PBS or cell medium. To undertake an additional evaporative densification step, the rod-tube assembly was suspended horizontally and rotated slowly under a biological safety cabinet for 1 h to allow for air drying.

2.3. Second-harmonic Generation Imaging of Tube Samples

Planar strips of collagen were cut from the full length of the tubes. Samples were mounted between two #1.5 glass coverslips, supported by a silicone spacer, and the coverslip ends were taped together. An inverted Leica TCS SP5 acousto-optic beam splitter (AOBS) multiphoton laser scanning microscope equipped with a Modelocked Ti:Sapphire Laser was used for second-harmonic generation (SHG) imaging, with the excitation laser (Ti:Sapphire) tuned to 880 nm. At this specific excitation wavelength, the wavelength of the emitted SHG signal was at 440 nm. A 20x objective was used to focus the excitation beam on the sample and to collect backscattered emission signals which are delivered through the AOBS and the fully opened confocal pinhole (600 µm) to the spectral detection system (descanned pathway). Highly specific SHG images were obtained through a 430-450 nm emission bandwidth channel detected on a hybrid detector. Tiled images were subsequently analysed using ImageJ.

2.4. Genipin Crosslinking

Genipin (Bioserv UK) was resuspended in sterile PBS at 1 and 10 mM concentrations. Samples of densified collagen tube were immersed in genipin solutions and placed on an orbital shaker for 24 h at room temperature, followed by a further 24 h in sterile PBS. Biocompatibility testing of 1 mM genipin solutions with collagen tubes seeded with cells was performed using cell medium containing dissolved genipin. Tubes were immersed in cell medium containing genipin and left in an incubator at 37 °C for 24 h.

2.5. Burst Pressure Testing

The burst pressure of 10 mM genipin crosslinked tubes, with a lumen diameter of 5 mm and wall thickness of 1.5 mm, was measured. An industrial pressure sensor (rated to 50 psi, Mouser Electronics) and a 5 mL syringe were interfaced

to the collagen tubes via a pair of stainless steel tubes supported by a pair of machined adapter pieces (Figure S1(a)). To generate a good seal, heat shrink tubing (RS Components) was positioned onto the steel surface and the collagen tube placed over this. A further layer of heat shrink tubing was heated onto the ends of the tube to create a good seal. A gap of 20 mm was maintained between the stainless steel tube interface at each end. The custom-made pressure measurement control system (Figure S1(b)) consisted of an instrumentation amplifier, Arduino process controller and serial data logger software (Termite). Pressure generated by a water-filled syringe was ramped up gradually until the tube burst, and the maximum pressure at the burst point recorded. 3 samples were tested per group.

2.6. Suture Retention Testing

The forces during suture pullout of 10 mM genipin crosslinked tubes, with a lumen diameter of 5 mm and wall thickness of 1.5 mm, was measured using an Instron desktop testing machine, fitted with a 5 N load cell. Unwrapped collagen tube samples, consisting of 10 mm x 5 mm sections, were clamped at the edge located opposite to the suture. A 7-0 polypropylene suture was threaded through the specimens (using a swaged needle) and both ends of the suture gripped into another clamp. The suture hole was centred with respect to the specimen width and its distance from the specimen end was 2 mm. The crosshead displacement was measured using a linear variable differential transformer (LVDT). Tests were conducted in displacement control at a rate of 3 mm/min until final failure, characterised by suture pullout. 3 samples were tested from each group.

2.7. Solubility Tests

Representative samples cut from uncrosslinked and genipin-crosslinked densified collagen tubes, alongside samples of excised pig vena cava (Medical Meats), were immersed in 100 mM acetic acid solution. A change in mass was measured over a 2 h period for uncrosslinked samples and over several days for crosslinked tube and excised vena cava samples, using a mass balance with a precision of 0.1 mg and removing the fluid at regular timepoints. However, as the uncrosslinked samples swelled and dissolved, it was not possible to reliably remove all the surrounding fluid without also removing the dissolving collagen.

2.8. Cell Culture and Characterisation

Human liver cancer cells (HepG2s) were cultured in DMEM+10 % FBS. Green fluorescent protein (GFP) and Red Fluorescent Protein (RFP) human umbilical vein endothelial cells (HUVECs, Promocell), normal human lung fibroblasts (NHLFs, Promocell) and mesenchymal stem cells (MSCs, Promocell) were cultured in their respective proprietary mediums (Promocell). Smooth muscle cells (SMCs) were derived from human embryonic stem cells (H9) via the neural crest or lateral plate mesoderm intermediates using established protocols [41, 42] and were subsequently cultured in standard medium (DMEM+10 % FBS). Cells were cultured until 90% confluency and detached from T75 flasks using TrypLE (Life Technologies), and subsequently centrifuged at 250 g for 5 min and counted using a haemocytometer.

Densification experiments where cells were encapsulated into the walls of the tubes were performed at 2-8 × 10^6 cells per tube (i.e. 1-4 × 10^5 cells/mL for 20 mL precursor solution), using collagen tubes with luminal diameters of 2 and 5 mm. Tubes with cells encapsulated in the bulk were prepared using either HepG2s, NHLFs, GFP HUVECs and RFP HUVECs, or SMCs. The collagen precursor solution was prepared as above, subtracting a volume for the addition of cells later, and was subsequently centrifuged at 4000 g for 10 min. 2-3 mL of collagen, without cells, was poured into the funnel to fill the cylindrical section. Doing so prevents the clogging of the membrane with cells and results in all the cells being present in the final tubular construct. The resuspended cell pellet was then pipetted on top of the precursor gel solution. Using a sterile metal spatula, the cells were then slowly mixed into the gel precursor solution until uniform,

and the solution was then poured into the funnel assembly as described above. For experiments with cells seeded into the bulk of the collagen gel, the funnel assembly was transferred to a 37 °C incubator for rapid gelation.

For densified collagen tubes with two distinct cell domains, two 10 mL collagen precursor solutions were prepared. Prior to adding cells, 1.5 mL from each precursor solution was transferred into the chamber. GFP and RFP HUVECs were subsequently stirred into their respective precursor solutions and slowly poured into the chamber, one after the other. As with above, the funnel assembly was transferred to a 37 °C incubator straight after assembly to prevent sedimentation and cell mixing.

HepG2s were used for experiments where cells were seeded upon the luminal surface of the tubes. Using a two T75 flasks, two lots of 50×10^6 HepG2 cells were pelleted and resuspended in 50 µL of Dulbecco's Modified Eagle Medium (DMEM). The 2 mm luminal diameter collagen tube was cut to length using small scissors and a sterile metal 2 mm diameter dowel pin (Accu) was positioned in the lumen at one end. Immersing the tube in DMEM, cells were transferred to the tube using a 1 mL syringe fitted with a 27 G × 1.5 in needle (Medisave). The cell-ladened tube was left in a 37 °C incubator for 6 h and then a second volume of HepG2s was added. Over several days, the attached HepG2s proliferated on the luminal surface.

Cell characterisation was performed via calcein AM staining (Life Technologies). For bulk seeding experiments, the cells were either stained prior to encapsulation or after the densification process. Briefly, calcein AM was resuspended at 4 mM in PBS. Cells plated in T75 flasks, or cell-seeded tubes, were washed in PBS and incubated in a 4 µM calcein AM solution in PBS, at 37 °C for 20 min. For luminal surface seeding experiments, HepG2s were stained prior to seeding. Cell-ladened tubes were imaged using an epi-fluorescence microscope (Zeiss Axio-Observer.Z1).

2.9. Luminal surface patterning process

Inverse 3D printed wax models (Solidscape) were prepared using a standard method [43]. 20% (w/v) high bloom, porcine gelatin solution was poured into the wax moulds and degassed using a vacuum pump. A polished nylon rod, 2 mm in diameter with a cutaway section at one end with 0.5 mm diameter, was then fitted through the wax mould and the assembly left at 4 °C to allow for gelatin gelation. The construct was subsequently immersed in acetone solution to dissolve the 3D printed wax mould and washed in PBS. Following the axial densification protocol as above, the nylon rod, with patterned gelatin gel, was used as a replacement for the Perspex central rod. Once the collagen has gelled, the central rod can be rotated as described above. Following densification of the collagen gel, the tube with patterned gelatin was placed in a PBS bath at 37 °C to melt the gelatin and allow it to diffuse away.

3. RESULTS

3.1. Formation of densified collagen tubes using a novel densification process

Collagen hydrogel-based tubes were manufactured using a novel densification method. A collagen gel precursor solution was cast between into a chamber, and the water removed from the gel via hydrophilic nylon membranes at the bottom of the chamber (Figure 1(a)), leading to the densification and alignment of collagen fibrils in the gel (Figure 1(b)). A funnel-shaped chamber enabled a large volume of collagen gel to be densified into a defined cylindrical mould section below, as the water is removed through the bottom of the chamber (Figure 1(c-h)). The specific dimensions of the funnel and cylindrical section of the mould enable a wide range of different luminal diameters and wall thicknesses to be fabricated. Interestingly, as water is removed through the membranes at the bottom of the funnel, the solid phase of the collagen gel densifies down into the bottom cylindrical section while a large fraction of the liquid phase remains and accumulates above the densified collagen gel.

The membrane assembly, consisting of membranes with pore sizes of 1.2 and 0.45 µm, was used to anchor the collagen gel at the base of the funnel-cylinder mould and control the rate of water removal, while aligning the central rod in the chamber with a high degree of precision, which was necessary for fine and uniform wall thicknesses to be produced. If no membranes are used at the bottom of the chamber, the collagen gel rapidly contracts upwards leaving an air pocket behind, which has the effect of preventing any further water removal from the bulk volume of the hydrogel in the funnel section.

As water is removed from the bottom of the chamber, water percolates through the pores of the collagen hydrogel, leading to the contraction of the polymeric phase downwards into the cylindrical section and rearrangement of the collagen fibrils (Figure 1(e,h)). It is critical to this process that the collagen gel is free to move over the casting chamber surface, without mass transfer of water along the gel surface; thus, a layer of oil lubricant is applied to the inside of the funnel.

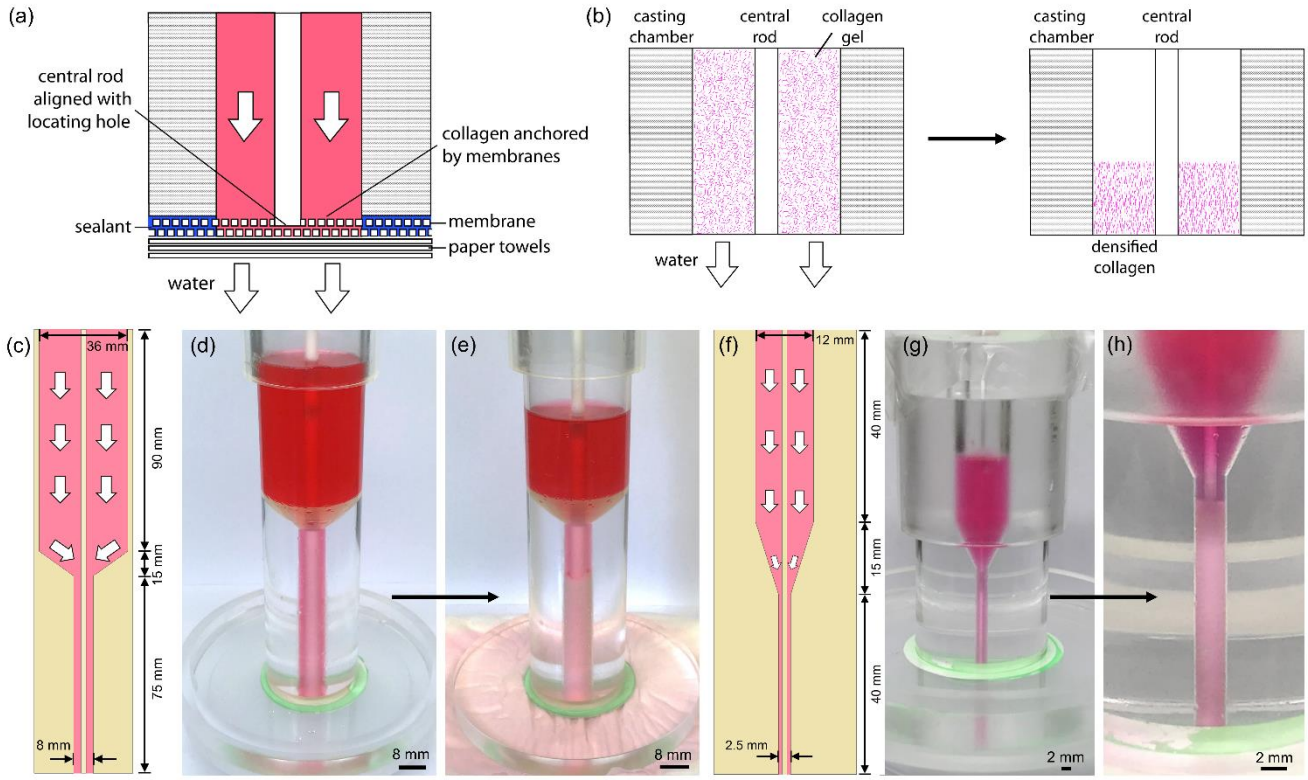

Figure 1: (a) Schematic depiction of the funnel base used for production of densified collagen tubes, showing the cylindrical section of the casting chamber, membrane configuration, central rod alignment, and water removal into paper towels. **(b)** Schematic showing axial densification of the collagen gel resulting in alignment of fibrils in the axial direction (i.e. long axis of the tubes). **(c)** Scale drawing of funnel used for generating collagen tubes with 5 mm luminal diameter and 1.5 mm wall thickness. **(d,e)** Funnel densification of 5 mm luminal diameter collagen tubes. The initial volume of collagen hydrogel was 60 mL. **(f)** Scale drawing of funnel used for generation collagen tubes with 1 mm luminal diameter and 0.5 mm wall thickness. **(g,h)** Funnel densification of 1 mm luminal diameter collagen tubes. The initial volume was 3 mL.

3.2. Genipin-crosslinking to improve mechanical strength and eliminate collagen dissolution

While the tubes display suitable mechanical strength for handling and cell seeding, crosslinking was investigated in order to imitate the mechanical strength of real tissue and eliminate any swelling and dissolution behaviour of collagen in acidic conditions (i.e. for clinical applications where the perfusate is acidic). Crosslinking was performed using genipin

at a biocompatible concentration of 1 mM, suitable in tubes where cells have been pre-seeded into the walls of the scaffold, or 10 mM, producing mechanically strong structures for burst pressure and suture retention testing.

3.3. Custom tubes fabricated de novo to a range of luminal diameters

Collagen tubes were manufactured over a range of lumen diameters and wall thicknesses. Tubes with luminal diameters of 5 mm and wall thickness of 1.5 mm (Figure 2(a)) were used for burst and suture testing. Tubes were manufactured using 2.5 and 5 mg/mL collagen gels. Increasing the starting volume of 2.5 mg/mL collagen gels led to proportionately longer tubes (Figure 2(a)(iii)). We also manufactured tubes with luminal diameters of 2 mm (Figure 2(b)), and 1 mm (Figure 2(c)). Wall thicknesses smaller than 0.5 mm were obtained using a further evaporative drying stage.

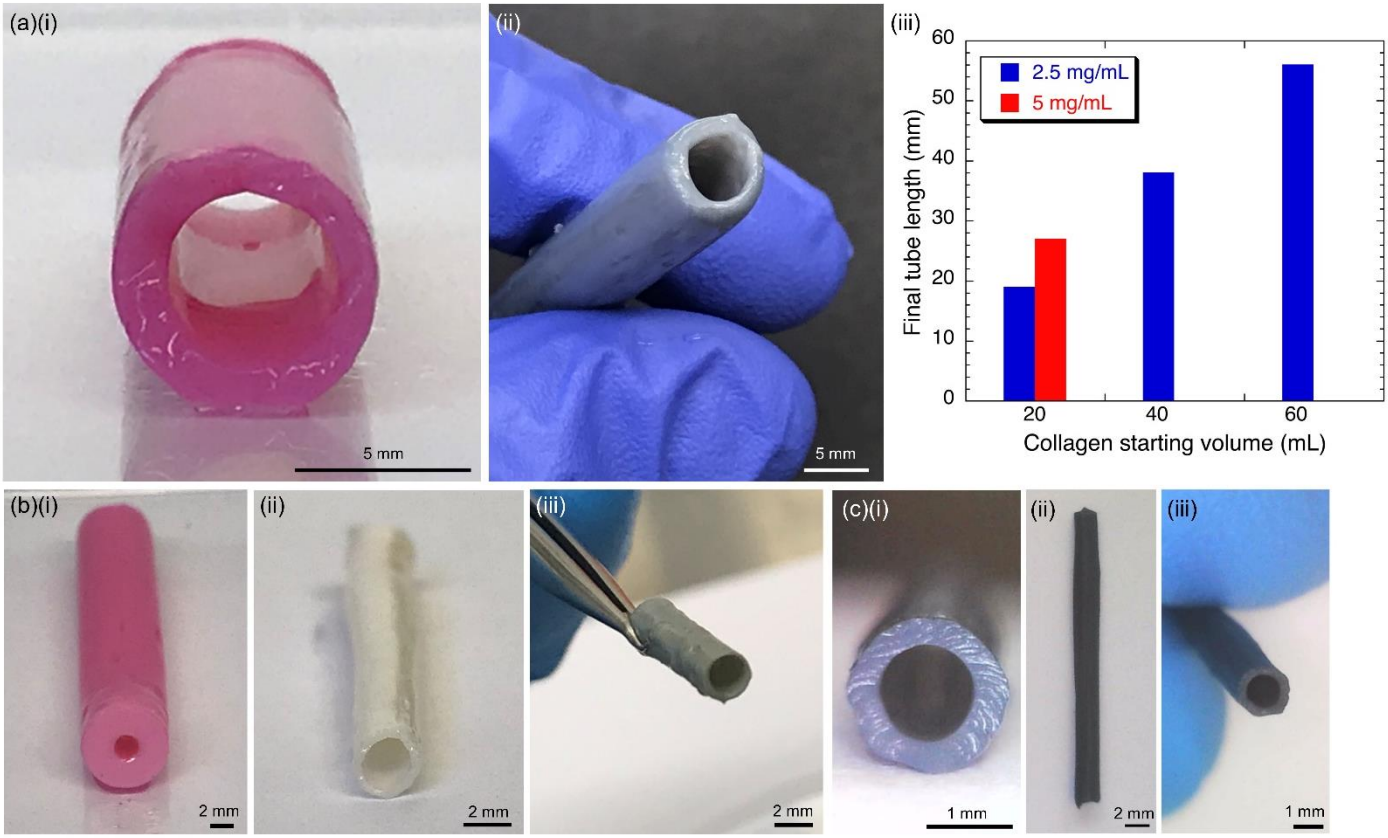

Figure 2: (a)(i) Uncrosslinked and **(ii)** genipin-crosslinked densified collagen tube with a 5 mm luminal diameter and 1.5 mm wall thickness. **(iii)** Tube length as a function of collagen gel starting volume and concentration. **(b)** Uncrosslinked densified collagen tube with **(i)** a wall thickness of 3 mm and **(ii)** a wall thickness of 0.5 mm, following air drying from initial 3 mm wall thickness. **(iii)** Genipin-crosslinked**,** 2 mm luminal diameter collagen tube. **(c)(i-iii)** 1 mm luminal diameter collagen tube with 0.2 mm wall thickness, following air drying from 0.5 mm wall thickness.

Attempts at air drying tubes without a prior axial densification step led to rips in the luminal surface and a non-uniform, mechanically weak tube. However, once the standard densification process is completed, the tubes have sufficient mechanical strength to be suspended from the central casting rod which makes it possible to air dry the tubes further to produce very small wall thicknesses. The degree of reduction in the wall thickness is a function of the starting collagen gel concentration and air-drying time. By employing a low starting collagen concentration, a 1 mm diameter tube could be manufactured with a wall thickness of 200 µm. This radial densification induces a further increase in the global collagen density, accompanied with a corresponding increase in mechanical strength. While the chamber densification method forms tubes with uniform wall thickness, evaporative drying can introduce variation in the wall thickness around the tube and so the tubes are rotated to support uniform drying from the surface. This is because air flow around the tube likely influences the rate of evaporative drying.

3.4. Measurement of burst pressures and forces during suture pullout

The maximum pressures at bursting point for 2.5 and 5 mg/mL collagen tubes (5 mm in diameter), crosslinked in a 10 mM genipin solution, are shown in Figure 3(a) and the peak forces during suture pullout for both collagen concentrations, normalised by the tube wall thickness, are shown in Figure 3(b). As expected, the 2.5 mg/mL tubes exhibit lower burst pressures and peak forces during suture pullout compared to the 5 mg/mL tubes. Figure 3a(iii) shows that the pressurised tubes fail due to a crack propagating in the axial direction (normal to the largest (hoop) stress). In the literature, results from suture pullout tests are often reported in terms of force, and therefore the values are influenced by the suture size and specimen geometry (e.g. a thicker collagen sample is expected to result in a larger peak force during pullout, for a given suture gauge). Furthermore, the loading rate can also affect the peak force values due to the time-dependent behaviour of the tested materials when undergoing deformation. Such variations in terms of test parameters hinder comparison with previous studies.

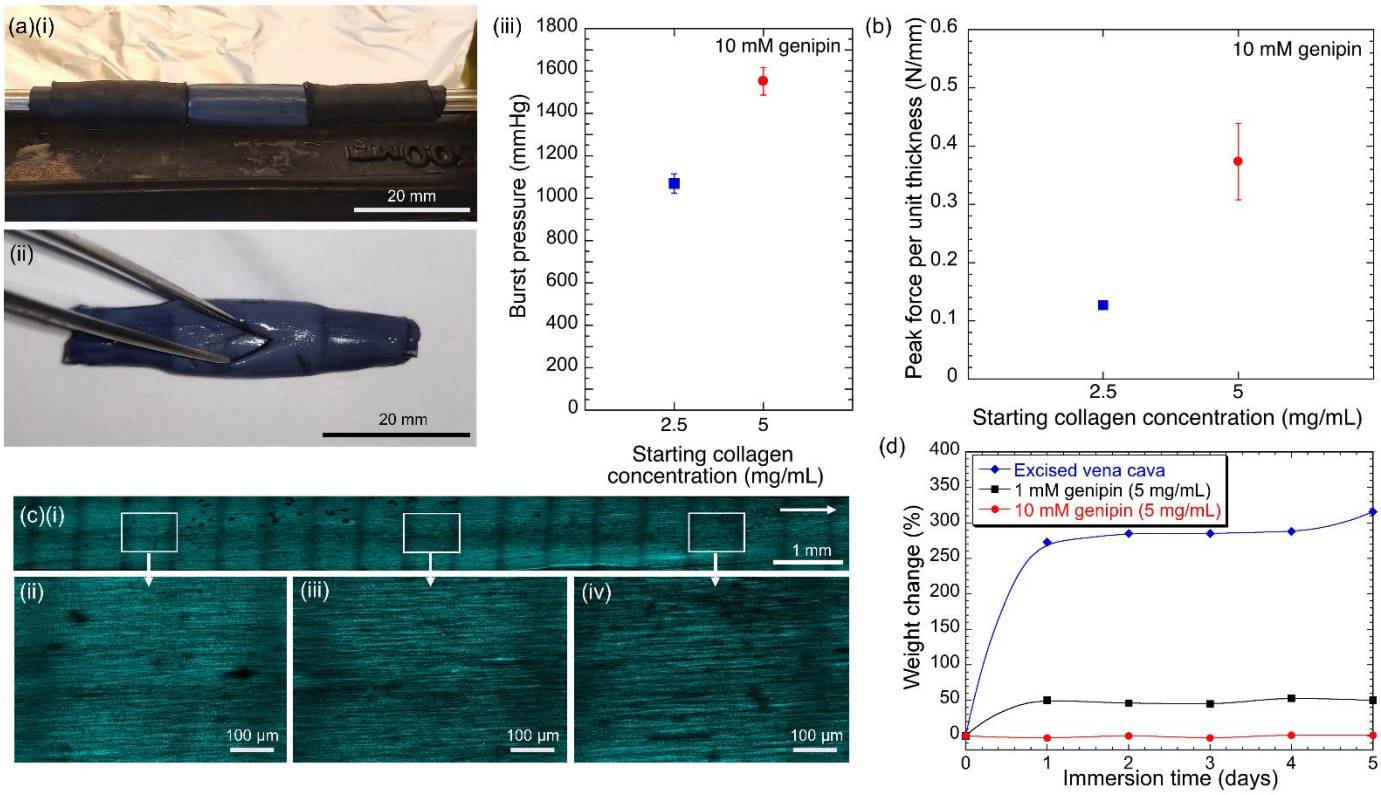

Figure 3: (a) Burst pressure testing for 10 mM genipin-crosslinked tubes; **(i)** setup showing the heat shrink tubing used to seal the ends, **(ii)** failed pressurised tube. **(iii)** Burst pressure as a function of starting collagen concentration (n = 3). **(b)** Suture retention for 10 mM genipin-crosslinked tubes, with 2.5 and 5 mg/mL starting collagen concentrations (n = 3). **(c)(i-iv)** Sample of collagen tube displaying fibre orientation and uniform fibre density, as shown using second harmonic generation microscopy. Arrow denotes axial direction (long axis of the tube) and insets show higher magnification cross-sections. **(d)** Acid solubility data obtained from immersion in 100 mM acetic acid solution showing percentage change in weight over a 5-day period for crosslinked tube samples and excised pig vena cava.

3.5. Collagen fibre orientation in tube wall

Second harmonic generation (SHG) imaging of the collagen tubular wall (Figure 3(c)) revealed that the fibres (bundles of densely packed fibrils) are aligned in the axial direction (i.e. the long axis of the tubes) and displayed a uniform fibre density.

3.6. Genipin-crosslinked densified collagen tubes are stable in acidic conditions

As expected, uncrosslinked samples of densified collagen tube swelled significantly when transferred from PBS to 100 mM acetic acid solution and dissolved within 2 h. However, once crosslinked with genipin, this dissolution behaviour was prevented. 1 mM genipin was sufficient to prevent the dissolution of the tubes, which underwent only limited swelling. Crosslinking with 10 mM genipin eliminated the swelling of the tubes entirely, as shown in Figure 3(d) over several days. These tubes were compared to excised, intact pig vena cava samples which, while not dissolving in acid, underwent a high degree of swelling over several days.

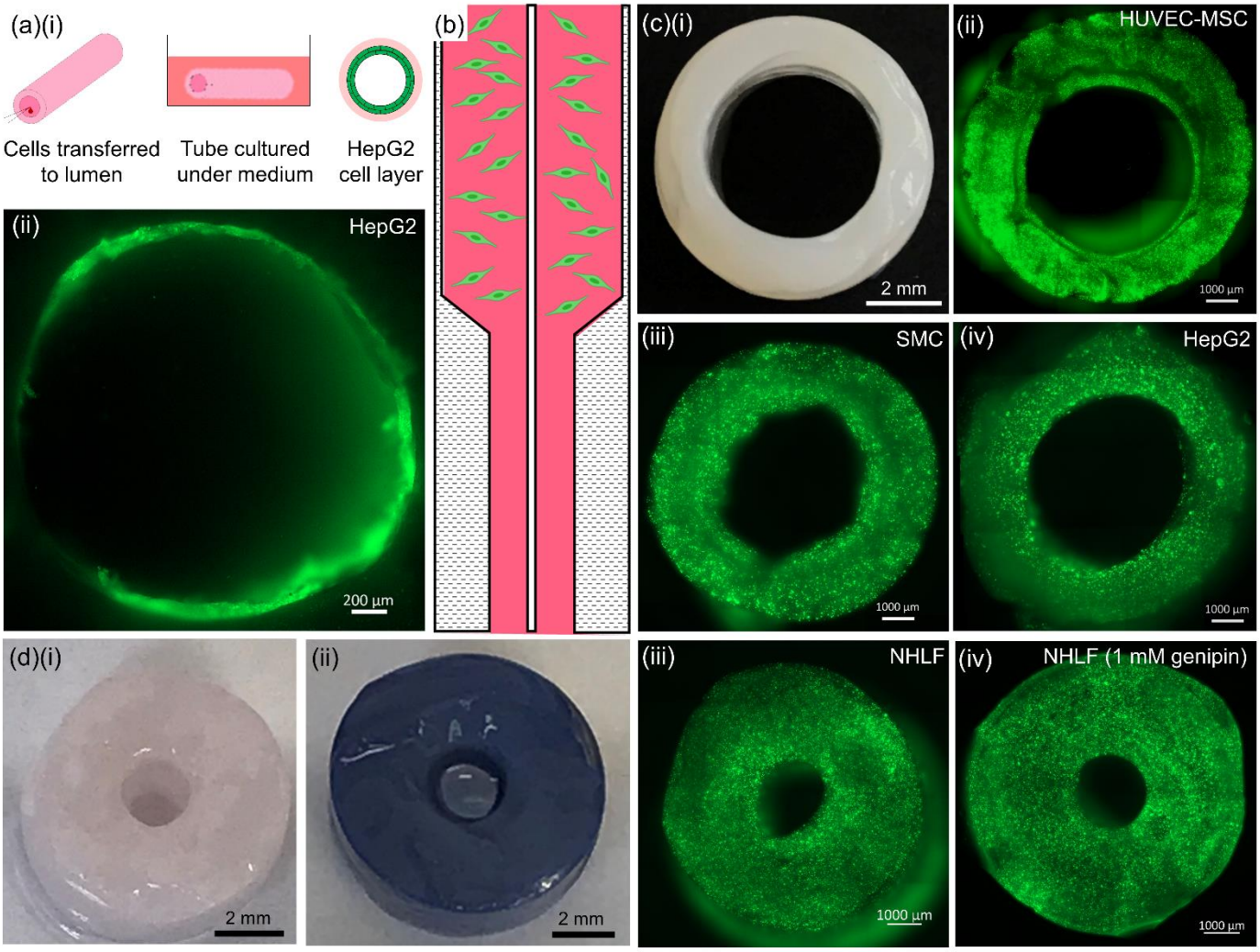

Figure 4: (a)(i) Schematic of surface seeding process. HepG2s were pipetted into lumen of tube and cultured under medium for 1 week. **(ii)** This led to formation of monolayer of cells on the luminal surface. **(b)** Schematic showing bulk cell seeding process. Cells were mixed into the funnel volume of the precursor gel solution. **(c)(i)** Cross-sectional image of 5 mm luminal diameter tube. **(ii)** HUVECs and MSCs, **(iii)** SMCs, and **(iv)** HepG2s were encapsulated into the walls of a 5 mm luminal diameter tube. **(d)** Samples of NHLF-seeded 2 mm luminal diameter tube **(i)** before and **(ii)** after 1 mM genipin crosslinking. NHLF-seeded 2 mm luminal diameter tubes showing high viability of cell population **(iii)** before and **(iv)** after 1 mM genipin crosslinking. All cells were stained using calcein AM (green).

3.7. Seeding of cells onto luminal surface and into walls of densified collagen tubes

Figure 4(a)(i) depicts a schematic representation of the surface seeding process. Immunofluorescent hepatic epithelial cells (HepG2s) were seeded onto the luminal surface of the collagen tubes and produced a monolayer structure after 1 week of culture Figure 4(a)(ii). In addition, cells were uniformly seeded into the walls of the densified collagen tubes through encapsulation in the initial undensified collagen gel as shown schematically in Figure 4(b). To demonstrate this,

experiments were undertaken in which populations of human umbilical vein endothelial cells (HUVECs) and mesenchymal stem cells (MSCs), normal human lung fibroblasts (NHLFs), or smooth muscle cells (SMCs) were added to the precursor collagen solution, which was subsequently gelled and densified overnight (Figure 4(c)(i-iv)). Sedimentation of these cells in the precursor gel solution was avoided by using 5 mg/mL collagen gel which had a suitable viscosity to slow this process and gelled rapidly upon heating to 37 °C. This yielded tubes in which cells were uniformly distributed through the walls of the tubes, for both 2 mm and 5 mm wall thicknesses. Genipin caused a significant colour change in the densified collagen tubes (Figure 4(d)). To test the biocompatibility of the crosslinker, a representative cellularised densified collagen tube (Figure 4(d)(iii))) was immersed in a 1 mM genipin solution for 24 h and showed that the cells maintained their viability (Figure 4(d)(iv)).

3.8. Generation of densified collagen tubes with two distinct cell domains

Disease modelling applications may require the formation of a densified collagen tube with two distinct regions consisting of two different cell types (e.g. two different types of smooth muscle cell). For these tubes, we used a mould with sloped walls (Figure 5(a)); we think the specific shape of the funnel could be important to generating different boundaries between the cell populations. Thus, tubes were manufactured casting half the precursor solution with one cell type and casting the second half of the precursor solution with the second cell type (Figure 5(b)).

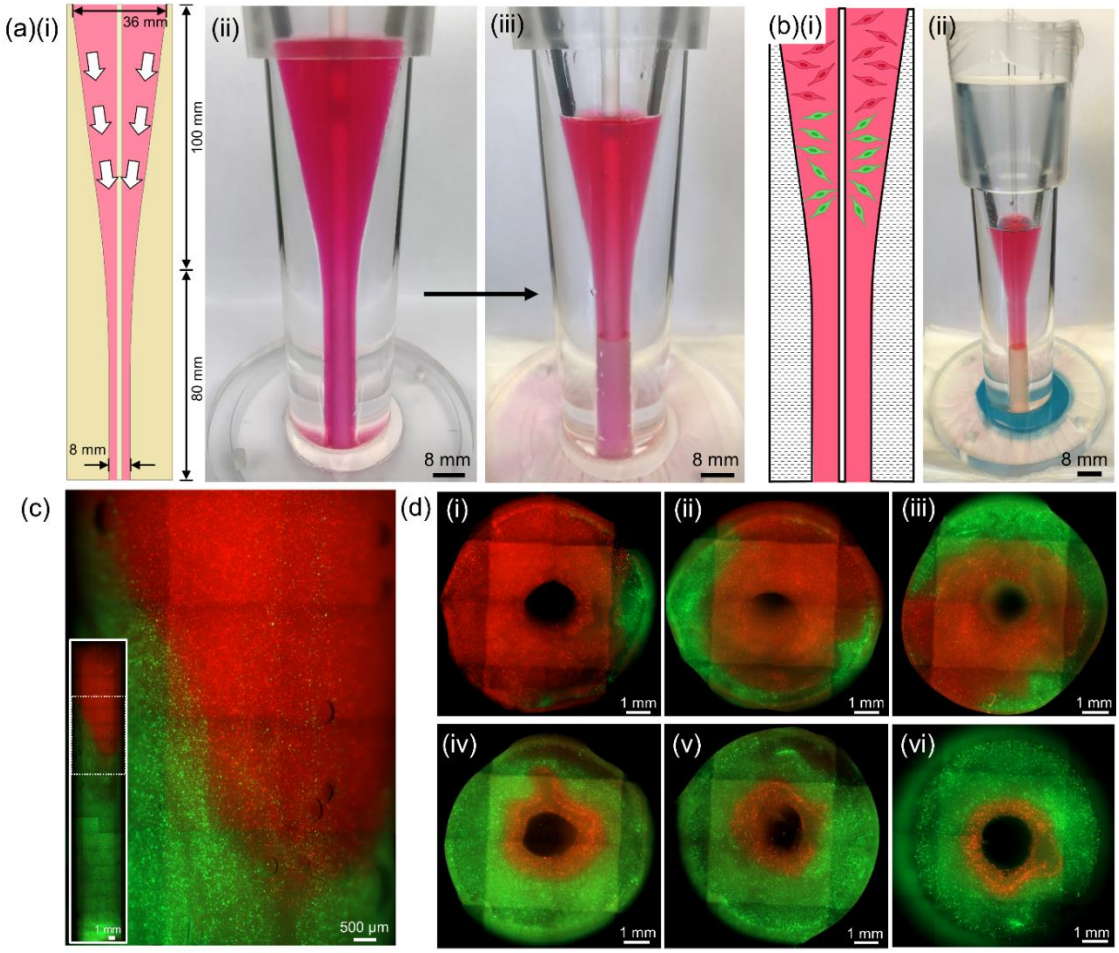

Figure 5: (a)(i) Scale drawing of sloped funnel for disease modelling applications. **(ii)** Before collagen densification and **(iii)** after densification. **(b)(i)** Schematic showing position of green and red fluorescently-labelled cells (GFP and RFP HUVECs respectively) in undensified collagen gel. **(ii)** Collagen tube manufacture with high density of fluorescent cells (in yellow). **(c)** Interface between two cell domains in densified collagen tube. Inset shows whole collagen tube. (**d)(i-vi)** Cross-sectional views moving down the densified collagen tube, showing transition from RFP to GFP HUVECs. Note that due to the densification process, RFP HUVECs are transformed from the top of the gel to wrap around the lumen, even in the GFP HUVEC region of the tube.

Cells from each sub-population were maintained in place by the high viscosity of the precursor gel solution prior to the gelation process. Cross-sectional views revealed two distinct cell domains consisting of either green or red fluorescently-labelled HUVECs (Figure 5(c)). Interestingly, the non-trivial mapping of the initial undensified collagen gel in the funnel section to the final densified collagen tube in the cylindrical section was such that the top group of HUVECs was located around the lumen while the bottom group of HUVECs populated the outer part of the walls, near the boundary between the cell domains (Figure 5(d)(i-vi)). The exact configuration of the cells in the final tube is likely determined by the exact angle of the sloped funnel and could be investigated further in the future. 2nd harmonic imaging of tubes formed using the sloped funnel is described in Figure S2.

3.9. Generation of densified collagen tubes with luminal surface patterning

Intestinal applications of the tubes may require the generation of crypt-villus structures on the luminal surface to promote efficient exchange of nutrients. To this end, we developed a process for patterning 3D printed structures in gelatin hydrogel (Figure 6(a)) which, following casting and densification of the collagen, generated a regular pattern of villi-like structures on the luminal surface, with cross-sections of 250 µm and heights of 500 µm (Figure 6(b-e)). However, large features height can hold up the densification process as the collagen fibrils is unable to deform around such features.

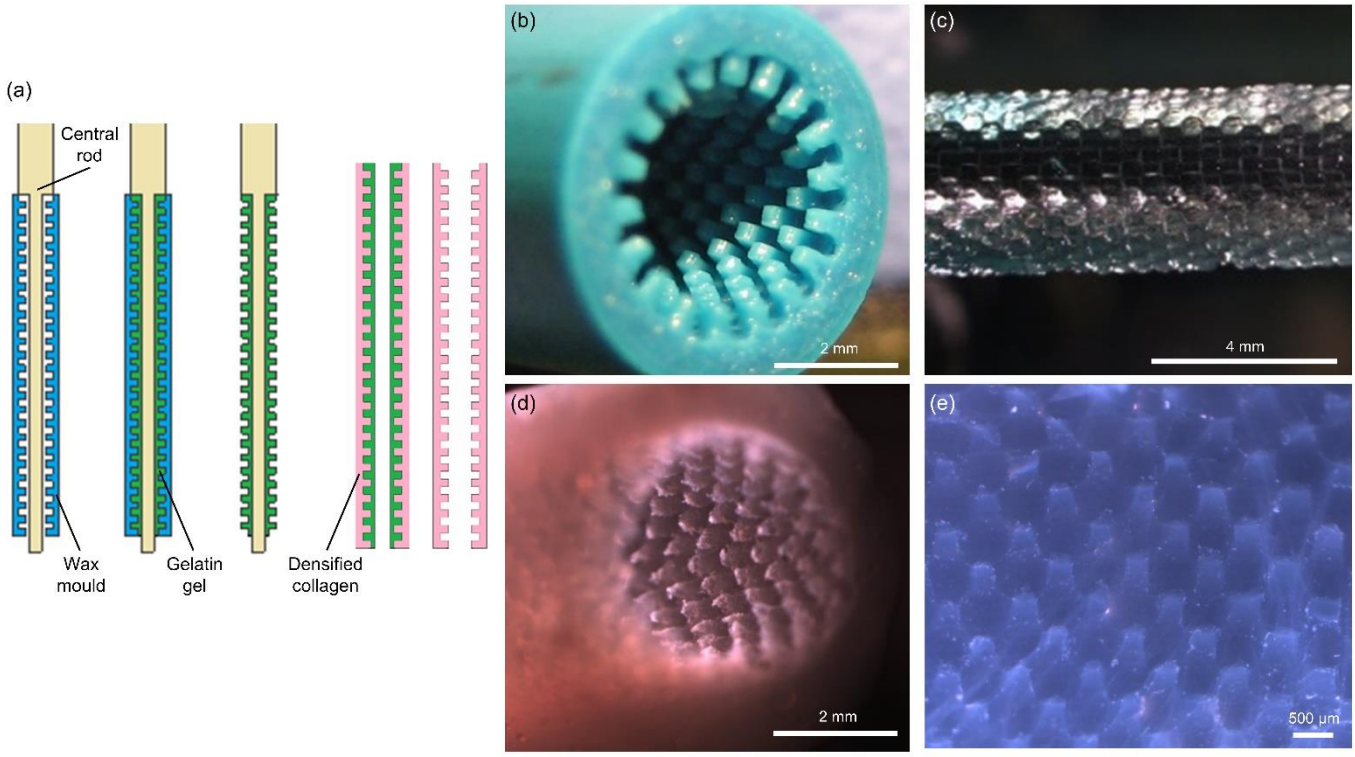

Figure 6: (a) Schematic showing luminal surface patterning process. Wax mould (blue) is mounted on a central rod with a cutaway. Wax mould is filled with gelatin gel (green) and the wax mould removed. After densification, the central rod is removed and the gelatin melted out of the densified collagen tube (pink). **(b)** 3D printed wax mould with patterned luminal features. **(c)** Gelatin gel inverse features, mounted on central rod. **(d)** Densified collagen tube with luminal surface features. **(e)** Luminal surface features at higher magnification.

4. DISCUSSION

Inadequate donor tissue supply to meet growing clinical need poses a significant problem to healthcare systems worldwide, supporting the generation of bioengineered vessels in the lab. A wide range of complex and patient-derived cellular structures, including organoids, can now be grown under 3D cell culture conditions, for tissues such as the coronary artery, bile duct, gastro-intestinal and genitourinary systems. However, there is a need to generate biomimetic, bioactive, and mechanically robust scaffolds on which to deploy these cells in a therapeutic clinical setting. The cellular

micro-environment of the scaffold must enable attachment, proliferation, differentiation, and ultimately, remodelling and replacement of the scaffold itself by native tissue. Further, scaffolds with a suitable mechanical strength and a perfusable vasculature will be required to meet this objective.

In solutions of neutral pH and sufficient ionic content, the collagen biopolymer is able, through multiple fibrillar self-assembly steps, to form a stable hydrogel consisting of solid phase fibrillar network and a trapped aqueous phase. These fibrils are capable of permanent reorganisation under an external stimulus, such as when the liquid phase of the gel is removed (e.g. by evaporation or percolation), which leads to a significant increase in the mechanical strength of the scaffold. Such a reduction in the percentage of water in the hydrogel would also more closely resemble the hydration level of real tissue. By extracting the aqueous phase, the gel undergoes a large and irreversible deformation, from an initial low density, random fibrillar state, to a high density, aligned fibrillar state [44, 45]. This syneresis is common to collagen gels; cells encapsulated in such gels impart forces upon the fibrillar structure which leads to the liquid phase being expelled from the gel [46, 47]. External, uniaxial loads applied to collagen gels also lead to expulsion of the liquid phase through the re-organisation of the fibrillar structure [48, 49]. In our process, the use of a particular funnel geometry, and membrane assembly with which to anchor the collagen gel, allows us to contract the collagen gel into a useful tubular construct and control the density and alignment of the collagen fibrils, which can produce tubes of a uniform density or density gradient along their length.

The final length of the collagen tubes was determined by several factors with the collagen gel starting volume, the ratio between the top funnel diameter and the bottom cylindrical diameter and the starting collagen concentration (2.5 mg/mL starting concentration and 20-60 mL starting volume, or 5 mg/mL and 20 mL). However, 2.5 mg/mL hydrogels were easier to cast without trapping air bubbles and underwent densification more rapidly. 5 mg/mL gels were used for cell experiments, where a rapid gelling and high viscosity were desirable to prevent cell deposition.

As shown when regions of collagen gel are labelled with two types of fluorescent cells, the particular mapping of volume elements from the funnel into the final cylindrical form is non-trivial; elements near the central rod are drawn down inside the surrounding gel due to the shape of the funnel. We also observe an expulsion of water from the top of the densifying gel (while we extract water from the base of the gel). As the collagen gel contracts downwards, it is likely due to the reorganisation of the fibrillar structure leads to water being forced out of the pores, which collects on top of the gel.

Through our densification process, collagen scaffolds can be fabricated to a wide range of diameters and wall thicknesses, consisting of highly aligned and bioactive collagen. The nature of the process allows for uniform cell encapsulation in the walls of the scaffold and onto the surface, enabling more complex cellular arrangements to be manufactured. Since the densification process reduces the volume of the gel significantly, the cell density can be substantially increased. Unlike other methods for producing collagen tubes, this process produces seamless vessels with a self-supporting lumen. Finally, we have shown that through minor modifications, additional features can be incorporated into the structure such as 3D printing-based luminal surface patterning, and that through sequential collagen casting, one can build a collagen gel scaffold with multiple cell domains, useful for future disease modelling.

Attempts at densifying collagen in a tall cylindrical mould failed presumably due to the high contact area between the collagen gel and the chamber producing large frictional forces, and also problems in maintaining the central rod in the centre of the chamber. The funnel geometry enables the densification process to be performed in a standard incubator, which allows for faster water removal and provides the suitable temperature and CO_2 environment for cell culture in the densifying collagen.

We investigated other materials for the casting chamber. Chambers fabricated using extrusion-based 3D printing had a very high surface roughness (owing to the layer-by-layer extrusion process) which led to very rough final tubes. Chambers made of PTFE failed to produce axial densification; instead, the collagen densified radially inwards. It is thought this was due to the very low friction surface allowing water to flow out of the gel along the funnel surfaces rather than through the collagen gel. Glass chambers allowed the oil layer to run off too easily and were expensive to manufacture.

While a density gradient may not be useful for tissue equivalent structures, the multi-domain tubes which make use of these slope-walled funnels may find future application as a means of studying aortic aneurysms. The spatial organisation of the domains near the boundary, with one type populating the region near the lumen and the other type populating the outer wall region, is highly reminiscent of the pattern of distribution of SMCs in the proximal aorta at the boundary between SMCs of neural crest and lateral plate mesoderm origins [50]. Indeed, this overlapping pattern is thought to be one of the reasons why aortic aneurysms and dissection are prevalent in the aortic root and ascending aorta [51]. Thus, this manufacturing technique may in future allow us to recreate the distinct cellular spatial configurations in the proximal aorta.

As future work, we intend to bind heparin onto the luminal surface of bioengineered collagen tubes which, along with a luminal cell layer, should control the thrombogenicity of the collagen-based construct, making it suitable for use in vascular tissue engineering. Subsequently we plan to implant the tubes into rats *in situ* as a replacement for a major blood vessel. It is likely that the densified collagen tubes can be implanted acellular, or soon after seeding with cells into the bulk gel and onto the luminal surface. However, for *in vitro* disease modelling and further maturation of the cellularized construct, the tubes can be mounted into a bioreactor culture rig. Culturing the tubes under such conditions will be investigated in future studies.

5. CONCLUSIONS

Tissue engineering seeks methods for the generation of tissue conduits for clinical replacement and disease modelling applications, which have suitable mechanical and biological properties. We have developed a novel method for the formation of densified collagen tubes *de novo* and at human length-scales with tissue-like mechanical strength which are highly customisable and seamless, into which cells can be uniformly seeded both into the walls and onto the luminal surface of the construct. Through genipin crosslinking, we are able to eliminate collagen swelling and dissolution in acidic conditions. We show that it is possible to form two distinct cell domains within the same densified collagen tube, displaying the complex mapping of collagen gel from an undensified to densified form. Finally, we report a method for luminal surface patterning of the densified collagen tubes to imitate physiological structures.

Author Contributions: AWJ and AEM designed research; AWJ conceived of, designed, and performed the densification method, analysed and interpreted associated results; AWJ, SB, SRE, AST: burst pressure and suture retention testing; AWJ, JO, AGC: cell experiments. AWJ and AEM prepared figures. AWJ wrote the main manuscript. KSP, SS, AEM: supervision. All authors gave final approval for publication.

Acknowledgements: Financial support for this work has come from the Engineering and Physical Sciences Research Council (EPSRC, EP/R511675/1), the Isaac Newton Trust and the Rosetrees Trust (M787). Financial support for AWJ and JO has been provided via EPSRC (EP/R511675/1) and a WD Armstrong Doctoral Fellowship, respectively. Support for SS via a BHF Senior Fellowship (FS/18/46/33663) is gratefully acknowledged. We wish to acknowledge Fadwa Joud

of the Cancer Research UK, Cambridge Institute for second harmonic generation microscopy of densified collagen tube samples, Peter J. Holt of the Wellcome‐Medical Research Council Cambridge Stem Cell Institute, for smooth muscle cell culture, Stefan Savage for machining the Perspex funnels, and Peter W. Justin for design and manufacture of the burst pressure measurement apparatus.

References

1. Hoenig MR, Campbell GR, Rolfe BE, Campbell JH. Tissue-engineered blood vessels: alternative to autologous grafts? Arterioscler Thromb Vasc Biol. 2005;25(6):1128-34.
2. L'Heureux N, Dusserre N, Konig G, Victor B, Keire P, Wight TN, et al. Human tissue-engineered blood vessels for adult arterial revascularization. Nat Med. 2006;12(3):361-5.
3. Seifu DG, Purnama A, Mequanint K, Mantovani D. Small-diameter vascular tissue engineering. Nat Rev Cardiol. 2013;10(7):410-21.
4. Huang AH, Niklason LE. Engineering of arteries in vitro. Cell Mol Life Sci. 2014;71(11):2103-18.
5. Song HG, Rumma RT, Ozaki CK, Edelman ER, Chen CS. Vascular Tissue Engineering: Progress, Challenges, and Clinical Promise. Cell Stem Cell. 2018;22(3):340-54.
6. Sampaziotis F, Justin AW, Tysoe OC, Sawiak S, Godfrey EM, Upponi SS, et al. Reconstruction of the mouse extrahepatic biliary tree using primary human extrahepatic cholangiocyte organoids. Nat Med. 2017;23(8):954-63.
7. Justin AW, Saeb-Parsy K, Markaki AE, Vallier L, Sampaziotis F. Advances in the generation of bioengineered bile ducts. Biochim Biophys Acta Mol Basis Dis. 2018;1864(4 Pt B):1532-8.
8. Hori Y, Nakamura T, Matsumoto K, Kurokawa Y, Satomi S, Shimizu Y. Tissue Engineering of the Small Intestine by Acellular Collagen Sponge Scaffold Grafting. The International Journal of Artificial Organs. 2001;24(1):50-4.
9. Grikscheit TC, Ochoa ER, Ramsanahie A, Alsberg E, Mooney D, Whang EE, et al. Tissue-engineered large intestine resembles native colon with appropriate in vitro physiology and architecture. Ann Surg. 2003;238(1):35-41.
10. Martin LY, Ladd MR, Werts A, Sodhi CP, March JC, Hackam DJ. Tissue engineering for the treatment of short bowel syndrome in children. Pediatr Res. 2018;83(1-2):249-57.
11. Poghosyan T, Catry J, Luong-Nguyen M, Bruneval P, Domet T, Arakelian L, et al. Esophageal tissue engineering: Current status and perspectives. J Visc Surg. 2016;153(1):21-9.
12. Arakelian L, Kanai N, Dua K, Durand M, Cattan P, Ohki T. Esophageal tissue engineering: from bench to bedside. Ann N Y Acad Sci. 2018;1434(1):156-63.
13. Atala A. Tissue engineering for the replacement of organ function in the genitourinary system. American Journal of Transplantation. 2004;4(s6):58-73.
14. Macchiarini P, Jungebluth P, Go T, Asnaghi MA, Rees LE, Cogan TA, et al. Clinical transplantation of a tissue-engineered airway. The Lancet. 2008;372(9655):2023-30.
15. O'Leary C, Gilbert JL, O'Dea S, O'Brien FJ, Cryan SA. Respiratory Tissue Engineering: Current Status and Opportunities for the Future. Tissue Eng Part B Rev. 2015;21(4):323-44.
16. Goh CS, Joethy JV, Tan BK, Wong M. Large animal models for long-segment tracheal reconstruction: a systematic review. J Surg Res. 2018;231:140-53.
17. Udelsman B, Mathisen DJ, Ott HC. A reassessment of tracheal substitutes-a systematic review. Ann Cardiothorac Surg. 2018;7(2):175-82.
18. Wangensteen KJ, Kalliainen LK. Collagen tube conduits in peripheral nerve repair: a retrospective analysis. Hand (N Y). 2010;5(3):273-7.
19. Chwalek K, Tsurkan MV, Freudenberg U, Werner C. Glycosaminoglycan-based hydrogels to modulate heterocellular communication in in vitro angiogenesis models. Sci Rep. 2014;4:4414.
20. McCoy MG, Wei JM, Choi S, Goerger JP, Zipfel W, Fischbach C. Collagen Fiber Orientation Regulates 3D Vascular Network Formation and Alignment. ACS Biomater Sci Eng. 2018;4(8):2967-76.
21. Wimmer RA, Leopoldi A, Aichinger M, Wick N, Hantusch B, Novatchkova M, et al. Human blood vessel organoids as a model of diabetic vasculopathy. Nature. 2019;565(7740):505-10.
22. Bennett MR, Sinha S, Owens GK. Vascular Smooth Muscle Cells in Atherosclerosis. Circ Res. 2016;118(4):692-702.
23. Granata A, Serrano F, Bernard WG, McNamara M, Low L, Sastry P, et al. An iPSC-derived vascular model of Marfan syndrome identifies key mediators of smooth muscle cell death. Nat Genet. 2017;49(1):97-109.
24. Jung Y, Ji H, Chen Z, Fai Chan H, Atchison L, Klitzman B, et al. Scaffold-free, Human Mesenchymal Stem Cell-Based Tissue Engineered Blood Vessels. Sci Rep. 2015;5:15116.
25. Norotte C, Marga FS, Niklason LE, Forgacs G. Scaffold-free vascular tissue engineering using bioprinting. Biomaterials. 2009;30(30):5910-7.
26. Quint C, Kondo Y, Manson RJ, Lawson JH, Dardik A, Niklason LE. Decellularized tissue-engineered blood vessel as an arterial conduit. Proc Natl Acad Sci U S A. 2011;108(22):9214-9.
27. Dahl SLM, Kypson AP, Lawson JH, Blum JL, Strader JT, Li Y, et al. Readily Available Tissue-Engineered Vascular Grafts. Science Translational Medicine. 2011;3(68):68ra9-ra9.
28. Kirkton RD, Santiago-Maysonet M, Lawson JH, Tente WE, Dahl SLM, Niklason LE, et al. Bioengineered human acellular vessels recellularize and evolve into living blood vessels after human implantation. Science Translational Medicine. 2019;11(485):eaau6934.

29. Tachibana M, Nagamatsu GR, Addonizio JC. Ureteral Replacement Using Collagen Sponge Tube Grafts. Journal of Urology. 1985;133(5):866-9.
30. Boland ED, Matthews JA, Pawlowski KJ, Simpson DG, Wnek GE, Bowlin GL. Electrospinning collagen and elastin: preliminary vascular tissue engineering. Frontiers in bioscience : a journal and virtual library. 2004;9:1422-32.
31. Nakamura T, Inada Y, Fukuda S, Yoshitani M, Nakada A, Itoi S, et al. Experimental study on the regeneration of peripheral nerve gaps through a polyglycolic acid-collagen (PGA-collagen) tube. Brain Res. 2004;1027(1-2):18-29.
32. Seliktar D, Black RA, Vito RP, Nerem RM. Dynamic Mechanical Conditioning of Collagen-Gel Blood Vessel Constructs Induces Remodeling In Vitro. Annals of Biomedical Engineering. 2000;28(4):351-62.
33. Brown RA, Wiseman M, Chuo C-B, Cheema U, Nazhat SN. Ultrarapid Engineering of Biomimetic Materials and Tissues: Fabrication of Nano- and Microstructures by Plastic Compression. Advanced Functional Materials. 2005;15(11):1762-70.
34. Isenberg BC, Williams C, Tranquillo RT. Small-diameter artificial arteries engineered in vitro. Circ Res. 2006;98(1):25-35.
35. Micol LA, Ananta M, Engelhardt EM, Mudera VC, Brown RA, Hubbell JA, et al. High-density collagen gel tubes as a matrix for primary human bladder smooth muscle cells. Biomaterials. 2011;32(6):1543-8.
36. Ghezzi CE, Marelli B, Muja N, Nazhat SN. Immediate production of a tubular dense collagen construct with bioinspired mechanical properties. Acta Biomater. 2012;8(5):1813-25.
37. Loy C, Laine A, Mantovani D. Rotation-based technique for the rapid densification of tubular collagen gel scaffolds. Biotechnol J. 2016;11(12):1673-9.
38. Li X, Xu J, Bartolák-Suki E, Jiang J, Tien J. Evaluation of 1-mm-diameter endothelialized dense collagen tubes in vascular microsurgery. Journal of biomedical materials research Part B, Applied biomaterials. 2020;108(6):2441-9.
39. Rajan N, Habermehl J, Cote MF, Doillon CJ, Mantovani D. Preparation of ready-to-use, storable and reconstituted type I collagen from rat tail tendon for tissue engineering applications. Nat Protoc. 2006;1(6):2753-8.
40. Tysoe OC, Justin AW, Brevini T, Chen SE, Mahbubani KT, Frank AK, et al. Isolation and propagation of primary human cholangiocyte organoids for the generation of bioengineered biliary tissue. Nat Protoc. 2019;14(6):1884-925.
41. Cheung C, Bernardo AS, Pedersen RA, Sinha S. Directed differentiation of embryonic origin-specific vascular smooth muscle subtypes from human pluripotent stem cells. Nat Protoc. 2014;9(4):929-38.
42. Serrano F, Bernard WG, Granata A, Iyer D, Steventon B, Kim M, et al. A Novel Human Pluripotent Stem Cell-Derived Neural Crest Model of Treacher Collins Syndrome Shows Defects in Cell Death and Migration. Stem Cells Dev. 2019;28(2):81-100.
43. Justin AW, Brooks RA, Markaki AE. Multi-casting approach for vascular networks in cellularized hydrogels. J R Soc Interface. 2016;13(125).
44. Liu Z, Toh W, Ng TY. Advances in Mechanics of Soft Materials: A Review of Large Deformation Behavior of Hydrogels. International Journal of Applied Mechanics. 2015;07(05):1530001.
45. Lai VK, Nedrelow DS, Lake SP, Kim B, Weiss EM, Tranquillo RT, et al. Swelling of Collagen-Hyaluronic Acid Co-Gels: An In Vitro Residual Stress Model. Ann Biomed Eng. 2016;44(10):2984-93.
46. Hadjipanayi E, Ananta M, Binkowski M, Streeter I, Lu Z, Cui ZF, et al. Mechanisms of structure generation during plastic compression of nanofibrillar collagen hydrogel scaffolds: towards engineering of collagen. J Tissue Eng Regen Med. 2011;5(7):505-19.
47. Ban E, Franklin JM, Nam S, Smith LR, Wang H, Wells RG, et al. Mechanisms of Plastic Deformation in Collagen Networks Induced by Cellular Forces. Biophys J. 2018;114(2):450-61.
48. Knapp DM, Barocas VH, Moon AG, Yoo K, Petzold LR, Tranquillo RT. Rheology of reconstituted type I collagen gel in confined compression. Journal of Rheology. 1997;41(5):971-93.
49. Tang Y, Ballarini R, Buehler MJ, Eppell SJ. Deformation micromechanisms of collagen fibrils under uniaxial tension. J R Soc Interface. 2010;7(46):839-50.
50. Sawada H, Rateri DL, Moorleghen JJ, Majesky MW, Daugherty A. Smooth Muscle Cells Derived From Second Heart Field and Cardiac Neural Crest Reside in Spatially Distinct Domains in the Media of the Ascending Aorta-Brief Report. Arterioscler Thromb Vasc Biol. 2017;37(9):1722-6.
51. Davaapil H, Shetty DK, Sinha S. Aortic "Disease-in-a-Dish": Mechanistic Insights and Drug Development Using iPSC-Based Disease Modeling. Front Cell Dev Biol. 2020;8:550504.